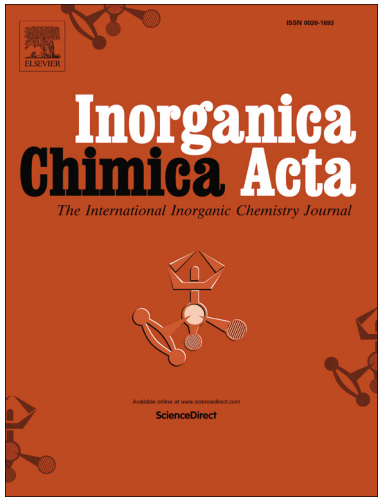

Research paper

Kinetics and mechanistic study of polynuclear platinum(II) polypyridyl complexes; A paradigm shift in search of new anticancer agents

Panyako Wangoli. Asman

PII: S0020-1693(17)30847-2
DOI: http://dx.doi.org/10.1016/j.ica.2017.08.065
Reference: ICA 17885

To appear in: *Inorganica Chimica Acta*

Received Date: 13 July 2017
Revised Date: 25 August 2017
Accepted Date: 30 August 2017

Please cite this article as: P.W. Asman, Kinetics and mechanistic study of polynuclear platinum(II) polypyridyl complexes; A paradigm shift in search of new anticancer agents, *Inorganica Chimica Acta* (2017), doi: http://dx.doi.org/10.1016/j.ica.2017.08.065

Full Title	**Kinetics and mechanistic study of polynuclear platinum(II) polypyridyl complexes; A paradigm shift in search of new anticancer agents**
Article type	Research paper
Keywords:	Reactivity, rigidity, flexibility, methylene, associative
Corresponding author	Panyako Wangoli. Asman, Ph.D. University of KwaZulu-Natal, 3209, Scottsville, Pietermaritzburg, South Africa E-mail: pwangoli@yahoo.com Cell-phone: +254720383345
Corresponding author's institution	University of KwaZulu Natal
Abstract	This paper reports on a mechanistic interaction between mononuclear and polynuclear platinum(II) complexes *viz;* phenyl-dichlorido-2,2'-dipyridinylaminediaquaplatinum(II) (**PtC1**); di-2-pyridylaminomethylbenzenediaquaplatinum(II) (**PtC2**); 1,3,5-tris(2,2'dipyridylamino)-benzenehexaquaplatinum(II) (**PtC3**); 1,3,5-tris(2,2'dipyridylmethylamino)benzenehexaquaplatinum(II) (**PtC4**); and 2,4,6-tris(2,2'-dipyridylamino)-1,3,5-triazinehexaquaplatinum(II) (**PtC5**) with thiourea nucleophiles under *pseudo*-first-order conditions as a function of nucleophile concentration and temperature using stopped-flow and UV-Vis spectrophotometric techniques. The reactivity of the complexes followed the order **PtC5 > PtC1 > PtC3 > PtC2 > PtC4** with thiourea (TU) as the entering nucleophile. The study demonstrates that both rigidity and flexibility has an influence on the kinetics of the complexes and governs by both steric and electronic effects. Introduction of methylene groups destroys conjugacy and lowers the acidity of the complexes. Kinetic and DFT data concur and illustrates that electron donation by methylene bridge leads to stabilization of the complexes. The study further shows that replacement of the methyne (=CH-) groups with nitrogen atoms enhances reactivity. The small positive enthalpy of activation and large negative values of entropy of activation indicate an associative mode of activation for aqua ligand substitutions and dechelation processes.

Kinetics and mechanistic study of polynuclear platinum(II) polypyridyl complexes; A paradigm shift in search of new anticancer agents

Panyako Wangoli. Asman*
School of Chemistry and Physics University of KwaZulu-Natal, 3209, Scottsville, Pietermaritzburg, South Africa
E-mail: pwangoli@yahoo.com

Abstract

This paper reports on a mechanistic interaction between mononuclear and polynuclear platinum(II) complexes *viz;* phenyl-dichlorido-2,2'-dipyridinylaminediaquaplatinum(II) (**PtC1**); di-2-pyridylaminomethylbenzenediaquaplatinum(II) (**PtC2**); 1,3,5-tris(2,2'dipyridylamino)-benzenehexaquaplatinum(II) (**PtC3**); 1,3,5-tris(2,2'dipyridylmethylamino)benzenehexaquaplatinum(II) (**PtC4**); and 2,4,6-tris(2,2'-dipyridylamino)-1,3,5-triazinehexaquaplatinum(II) (**PtC5**) with thiourea nucleophiles under *pseudo*-first-order conditions as a function of nucleophile concentration and temperature using stopped-flow and UV-Vis spectrophotometric techniques. The reactivity of the complexes followed the order **PtC5 > PtC1 > PtC3 > PtC2 > PtC4** with thiourea (**TU**) as the entering nucleophile. The study demonstrates that both rigidity and flexibility has an influence on the kinetics of the complexes and governs by both steric and electronic effects. Introduction of methylene groups destroys conjugacy and lowers the acidity of the complexes. Kinetic and DFT data concur and illustrates that electron donation by methylene bridge leads to stabilization of the complexes. The study further shows that replacement of the methyne (=CH-) groups with nitrogen atoms enhances reactivity. The small positive enthalpy of activation and large negative values of entropy of activation indicate an associative mode of activation for aqua ligand substitutions and dechelation processes.

Introduction

The search for more efficacious Pt-based drugs other than cisplatin has been amplified due to the steady rise in cancer deaths globally.[1,2] The clinical use of cisplatin and its analogous is restricted by dose-limiting deleterious side effects such as nausea, ototoxicity, nephrotoxicity, neurotoxicity, myelosuppression, and acquired resistance.[3-5] This search has been extended to multinuclear platinum(II) complexes such as BBR3464 and *N,N,N',N',N'',N*''-hexakis(2-pyridylmethyl)-1,3,5-tris(aminomethyl)-benzene which have shown cytotoxicity in some cell lines.[6-8] This class of complexes [multinuclear Pt((II)] has distinctive mechanisms of action compared to mononuclear analogues.[9,10] They have shown the potential to expand the spectrum of treatable tumours and to overcome clinical resistance in cisplatin cell lines.[11-13] Their increased cytotoxicity is due to different types of intra- and interstrand DNA cross-linking adducts which they form.[14,15] This is due to their ability to form flexible, non-directional and mainly interstrand DNA-adducts that enhances conformational changes that leads to improved antitumour activity.[16,17] This improved antitumour activity has made them a class of clinically relevant drug candidates.[18,19] The distinct molecular characters of pharmacological action of multinuclear complexes is contributed by the rigidity/flexibility of the bridging ligands in conjunction with the intra-metal distances that offer the possibility of forming both intra- and inter-strand DNA cross-linking adducts. The presence of more than one platinum centre causes formation of multiple adducts that disrupt DNA's helical structure with improved replication and transcription.[20,21] This is promoted by multinuclear Pt(II) complexes having appropriate metal-metal separation which is significant in polymetallic biosites. This improved mutagenicity is integrated to reach maximum level due to synergy of linking metal moieties.

In the development of the proposed antitumour agents, this study utilized 2,2'-dipyridylamine as the core chelating agent to synthesize multi and mononuclear Pt(II) analogues. The influence of this ligand on the reactivity of Pt(II) complexes and the ligand's ability to modulate the potential toxicity[22] of the metal complexes is of interest. Both mononuclear and multinuclear Pt(II) and Pd(II) complexes based on this core have showed high cytotoxicity as potential anticancer agents[23-25] which shows an area full of prospects that can be explored to give potential anticancer drug candidates. They form complexes with *cis* configuration similar to cisplatin which are likely to produce similar array of adducts with DNA but with improved biological consequences than cisplatin.[26] This study focuses on *cis* conformers since

cis/*trans* structure-activity relationship of platinum antitumor complexes, exemplified by cisplatin shows that only the *cis* geometry is therapeutically active. The complexes are designed by tuning the steric and electronic effects on reactivity. It is projected that such tuning of the lability of antitumour Pt(II) complexes may improve the efficacy and overcome the side effects of the present anticancer agents. The complexes designed herein are good models for mechanistic and kinetic studies and suggest potential prospects as anticancer drugs with *N*-donor ligands.[27] The study further tunes the complexes by incorporating methylene groups and heteroanalogues of benzene by replacing =CH- units with isovalent atoms of nitrogen. Such tuning of the linker remains vital to determine the influence of nitrogen on cytotoxicity of antitumour agents and as a π-acceptor atom on the reactivity of metal complexes.[28] In corporation of such chelating ligands that can interact with free or protein bound metal ions is important in understanding mechanistic activities of newly designed chemotherapeutics. The scope of this ligand substitution reactions is to determine the rate laws consistent of Pt(II) complexes which offer two labile reaction sites in nucleophilic medium. The study focuses on mechanistic overview based on experimental and computational calculations.

To gain insight into the mechanistic substitution reactions of these polynuclear Pt(II) complexes with biological nucleophiles, *viz* thiourea (**TU**), *N,N*'-dimethylthiourea (**DMTU**) and *N,N,N*',*N*'-tetramethylthiourea (**TMTU**), a full kinetic and mechanistic investigation was undertaken. The study determined the kinetics and bioactivity of trinuclear Pt(II) complexes with 6-aqua ligands with sulphur donor molecules for the first time. The nucleophiles studied are of special interest as they represent targets and competitors of anticancer platinum-based therapeutics in the cellular cell lines and also play a role as chemoprotective agents.[29,30] The specific roles of these nucleophiles has been outlined in the previous paper.[31] To achieve this objective, the study determined the influence of structural flexibility and rigidity on reactivity of complexes shown in Scheme 1. All the complexes are ligated by 2'2-dipyridylamine backbone that ensures a similar structure to cisplatin. However, the ancillary ligands are varied to investigate their influence on their substitution reactions. Such tailoring of the backbone linker is anticipated to improve bio-stability and bioavailability of these trinulear Pt(II) complexes as anti-tumour agents. Hence the goal of this investigation is to contribute towards a mechanistic understanding of the interaction of multinuclear Pt(II) complexes with biologically relevant molecules. This is due to multinuclear Pt(II) complexes showing wider spectrum of

activity that has given hope of forming clinically relevant candidates. This makes this class of complexes the most promising alternatives to cisplatin since they can provide significant cytostatic activity in several cisplatin resistant tumour cell lines. This paper shows how tailoring the backbone of the metal complex leads to dramatic changes in their acidity and reactivity. This tailoring of the bridging ligands is envisaged to provide special delivery carriers to selectively transport metal-based agents tumour cell-lines.

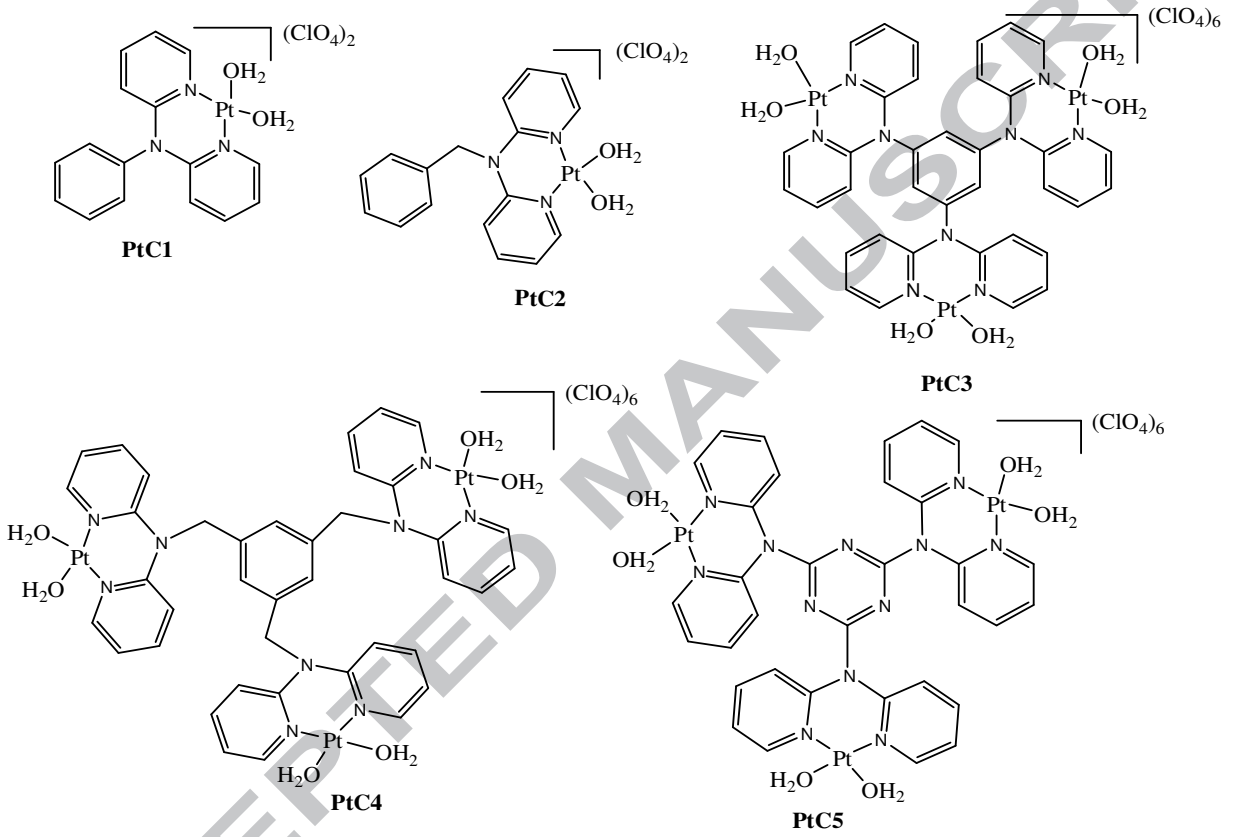

Scheme 1: Schematic structures and abbreviations for the aqua Pt(II) complexes.

Experimental Section

Materials and methods

All starting materials were obtained from commercial sources and used as received without further purification. The nucleophiles **TU**, 99 %, **DMTU**, 99 % and **TMTU**, 98 %, benzyl bromide, 98 %, bromobenzene, 99 %, cyanuric chloride (2,4,6-trichloro-1,3,5-triazine), 99 %, 1,3,5-tribromobenzene, 98 % and 1,3,5-tris(bromomethyl)benzene, 97 %, $AgClO_4$ 99.99 %, were obtained from Sigma Aldrich while K_2PtCl_4 and 2,2'-dipyridylamine (dpa) were obtained from Strem chemicals. De-ionized water was used in all experiments.

Synthesis of ligands

Three ligands; **di-2-pyridylaminobenzene, di-2-pyridylaminomethylbenzene**, and **1,3,5-tris(bromomethyl)benzene** were synthesized according to literature procedures.[32,33a] A weighed amount of bromoalkyl halide (0.855 g, 5.00 mmol) was dissolved in 3 mL DMF at room temperature and 2,2'-dipyridylamine (0.856 g, 5.00 mmol) and KOH (1.137 g, 20.26 mmol) in 5.00 mL DMF added drop wise. The resulting solution was stirred under nitrogen at room temperature for 24 hours and dried under vacuum. The residue was washed with water and extracted into $CHCl_3$ (3×50 mL). The extracts were dried over anhydrous sodium sulphate and filtered. The filtrate was dried under vacuum and chromatographed on silica gel with $CHCl_3$:CH_3OH (5:1) v/v. The resulting yellow product was recrystallized from an acetone-water mixture.

1,3,5-Tris(di-2-pyridylaminomethyl)benzene was prepared by reacting di-2-pyridylamine (0.856 g, 5 mmol) with potassium hydroxide (1.121 g, 20 mmol) in 5 mL of DMSO. The mixture was stirred for 1 hour and 1,3,5-tris(bromomethyl)benzene (0.595 g, 1.667 mmol) added and stirred for an additional 48 hours. Water was added drop-wise to induce crystallization. On standing, a yellow powder formed and was filtered off, washed with plenty of water and recrystallized from an ethyl acetate-petroleum ether mixture. The synthesized ligands were characterized using ^1H, ^{13}C NMR, mass spectrometry and elemental analysis.

Di-2-pyridylaminobenzene, Yield, 0.604 g, (49 %). ^1H NMR (400 MHz, $CDCl_3$, 303 K) δ 8.28 (2H, d, py), 7.68 (2H, t, py), 7.60 (2H, d, py), 7.57 (2H, d, ph), 7.20 (1H, t, ph), 7.16 (2H, d, ph), 6.94 (2H, t, py) ppm. ^{13}C NMR (100 MHz, $CDCl_3$, 303 K) δ 157.5, 148.6, 139.5, 117.4, 112 ppm. Anal. Calcd. for $C_{16}H_{13}N_3$, C, 78.13, H, 5.79, N, 16.08, Found C, 78.34, H, 5.45, N, 16.34; TOF MS ES^+ *m/z:* $[M+H]^+ = 248.309$.

Di-2-pyridylaminomethylbenzene, Yield, 0.277 g, (21 %). ^1H NMR (400 MHz, $CDCl_3$, 303 K) δ 8.40 (2H, d, py), 7.60 (2H, t, py), 7.37 (2H, d, py), 7.27 (2H, d, ph), 7.20 (1H, t, ph), 7.16 (2H, d, ph), 6.94 (2H, t, py), 5.55 (2H, s, CH_2) ppm, ^{13}C NMR (100 MHz, $CDCl_3$, 303 K) δ 157.5, 148.6, 139.8, 137.4, 128.0, 117.4, 114.4, 51.3 ppm. Anal. Calcd for $C_{17}H_{15}N_3$, C, 78.13, H, 5.79, N, 16.08, Found C, 77.78, H, 5.55, N, 16.48, TOF MS ES^+ (*m/z)*: $[M+H]^+ = 262.134$.

1,3,5-tris(di-2-pyridylaminomethyl)benzene, Yield, 0.578 g (55 %). For $C_{39}H_{33}N_9$, ^{1}H NMR (400 MHz, $CDCl_3$, 303 K) δ 8.22 (6H, d, py), 7.40 (6H, t, py), 7.09 (3H, s, ph), 6.92 (6H, d, py), 6.81 (6H, t, py), 5.34 (6H, s, CH_2) ppm. ^{13}C NMR (100 MHz, $CDCl_3$, 303 K) δ 157.4, 148.6, 139.5, 136.6, 124.0, 117.0, 114.5, 51.6 ppm. Anal. Calcd. for $C_{39}H_{33}N_9$, C, 74.67, H, 5.30, N, 20.10, Found C, 74.27, H, 5.12, N, 19.86, TOF MS ES$^+$ (m/z): $C_{39}H_{34}N_9^+$ = 628.2937.

1,3,5-tris(di-2-pyridylamino)benzene (tdab) was prepared according to literature procedure using 1,3,5-tribromobenzene and di-2-pyridylamine *via* copper-mediated Ullmann condensation.[34] A mixture of 1,3,5-tribromobenzene (0.525 g, 1.67 mmol) in dichloromethane (30 mL), di-2-pyridylamine (0.856 g, 5 mmol) in dichloromethane (20 mL), potassium carbonate (0.8976 g, 6.448 mmol) in water (10 mL) and copper (II) sulphate pentahydrate (0.1355 g, 0.5428 mmol) in water (10 mL) was stirred overnight at room temperature and evaporated to dryness under vacuum. The dried mixture was ground in a mortar and 5 drops of chloromethane added and heated at 210 ^{o}C for 8 hours under nitrogen. The mixture was cooled to room temperature and dissolved in a mixture of dichloromethane (50 mL) and water (50 mL). The organic layer was washed with water (3×50 mL), dried over Na_2SO_4, and concentrated to give a yellow residue that was purified by chromatographic column using tetrahydrofuran (THF) and hexane (3:1) v/v to obtain a brown solid. The brown solid was recrystallized from a mixture of CH_2Cl_2 – hexane to give a white crystalline compound.

1,3,5-tris(di-2-pyridylamino)benzene (tdab), Yield, 0.302 g, (57 %).^{1}H NMR (400 MHz, $CDCl_3$, 303 K) δ 8.28 (6H, d, py), 7.56 (6H, dd, py), 7.14 (6H, d, py), 6.91 (6H, dd, py), 3.16 (3H, s, ph) ppm, ^{13}C NMR (100 MHz, $CDCl_3$, 303 K) δ 158.0, 148.7, 146.8, 137.9, 120.6, 118.9, 117.9 ppm. Anal. Calcd for $C_{36}H_{27}N_9$: C, 73.83, H, 4.65, N, 21.52, Found C, 73.41, H, 4.81, N, 21.88.

2,4,6-tris(dipyridin-2-ylamino)–[1,3,5]-triazine (tdat) was prepared according to Gamez *et al.* method.[35] The synthesis was *via* sequential substitution of the three chlorides of cyanuric chloride by 2,2'-dipyridylamine. 2,4,6-trichloro-[1,3,5]-triazine (cyanuric chloride) (0.307 g, 1.67 mmol) was dissolved in 25 mL tetrahydrofuran (THF) and 3 equivalent moles of *N,N*-diisopropylethylamine (DIPEA, 'Hünig's base' 0.646 g, 5.00 mmol) added while stirring. The resulting yellow solution was cooled down to 0 ^{o}C. Subsequently, a solution of 2, 2'-dipyridylamine (0.856 g, 5.00 mmol) in THF (20 mL) was added drop-wise and the reaction

mixture stirred at 0 ^{o}C for 1 hour. The reaction mixture was warmed to room temperature and refluxed for 48 hours at 67 ^{o}C. The resultant white precipitate was isolated on a glass filter washed with THF (3×20 mL) and with ethanol (3×20 mL) to remove DIPEA.

2,4,6-tris(dipyridin-2-ylamino)–[1,3,5]-triazine (tdat), Yield 0.296 g (30 %). ^{1}H NMR (400 MHz, $CDCl_3$, 303 K) δ 8.35 (6H, d, py), 7.51 (6H, dd, py), 7.42 (6H, d, py), 7.03 (6H, dd, py) ppm, ^{13}C NMR (100 MHz, $CDCl_3$, 303 K) δ 165.8, 154.9, 148.2, 137.3, 122.9, 120.8 ppm. Anal. Calc. for $C_{33}H_{24}N_{12}$, C, 67.34, H, 4.11, N, 28.55, Found C, 66.98, H, 4.08, N, 28.80; TOF MS ES^{+} (m/z): $[M+Na]^{+}$ = 611.2141.

Preparation of PtC1, PtC2 and PtC4

The complexes were synthesized from their respective ligands according to a reported procedure.[36] A 50 mL solution of K_2PtCl_4 was stirred and the corresponding molar equivalent of respective ligands dissolved in a small amount of ethanol was added drop-wise. The reaction mixture was refluxed overnight at 50 °C. The resulting platinum(II) complexes were obtained as precipitates, washed with ultrapure water and diethyl ether and dried in vacuum overnight. They were characterized with similar techniques as ligands.

PtC1, Yield, 55 mg, (35 %). ^{1}H NMR (400 MHz, DMSO-d_6) δ 11.12 (s, 1H), 8.80(d, 3H), 7.96 (t, 3H), 7.28(d, 3H), 7.12 (d, 3H) ppm, ^{13}C NMR (100 MHz, DMSO-d_6) δ, 153.7, 148,6, 137.6, 117, 112.4 ppm, ^{195}Pt NMR -2105 ppm. Anal. Calcd. for $C_{16}H_{13}N_3PtCl_2$, C, 37.35, H, 2.55, N, 8.17, Found C, 37.52, H, 3.02, N, 7.84, TOF MS ES^{+}, *m/z:* $[M-Cl]^{+}$ = 479.0607.

PtC2, Yield, 69 mg, (44 %). ^{1}H NMR (400 MHz, DMSO-d_6) δ 8.83(d, 2H), 8.04 (t, 2H), 7.68(d, 2H), 7.53 (d, 2H), 7.36 (t, 1H), 7.26 (ddd, 4H), 5.43 (s, 2H) ppm, ^{13}C NMR (100 MHz, DMSO-d_6, 303 K) δ, 153.4, 151.7, 148.4, 141.3, 136.2, 129.2, 127.3, 117.8, 114.8, 53.7 ppm, ^{195}Pt NMR -2189.2 ppm. Anal. Calcd. for $C_{17}H_{15}N_3PtCl_2$, C, 38.72, H, 2.87, N, 7.97, Found C, 38.46, H, 3.07, N, 8.10; TOF MS ES^{+}, *m/z:* $[M+Na]^{+}$ = 550.0247.

PtC4, Yield, 120 mg, (53 %).^{1}H NMR (400 MHz, DMSO-d_6) δ 8.83(d, 6H), 8.04 (s, 3H), 7.74 (d, 4H), 7.30 (d, 14H), 5.34 (s, 6H) ppm, ^{13}C NMR (100 MHz, DMSO-d_6 303 K) δ, 153.5, 152.0, 141.5, 137.4, 127.3, 121.6, 116.8 and 53.9, ^{195}Pt NMR -2190.3 ppm. Anal. Calcd. for

$C_{39}H_{33}N_9Pt_3Cl_6$, C, 32.84, H, 2.33, N, 8.84, Found C, 32.36, H, 2.51, N, 8.60; TOF MS ES$^+$, *m/z:* $[M\text{-}Cl]^+$ = 1390.0830.

Synthesis of complexes PtC3 and PtC5 (tdabPt_3 and tdatPt_3)

These complexes were synthesized according to the procedure reported by Corey *et al.*[37,38] Synthesis of [$(PtCl_2)_3$(tdab) **PtC3**] and [$(PtCl_2)_3$(tdat) **PtC5**]: 93.9 mg (0.160 mmol) of tdat was dissolved in 6 mL CH_2Cl_2 and placed in a reaction tank. Benzene (4 mL) and a solution of K_2PtCl_4 (200 mg, 0.481 mmol) in a mixture of 3 mL of H_2O and 5 mL of DMSO were layered upon the solution of tdat in the reaction tank. The yellow K_2PtCl_4/H_2O/DMSO solution sank through the layer of benzene and settled upon the tdat/CH_2Cl_2 layer. The solvents were allowed to diffuse for two weeks at ambient temperature under nitrogen to dryness. Yellow crystalline solids were obtained weighed and characterized.

PtC3, Yield, 108 mg, (49 %). ^{1}H NMR (400 MHz, DMSO-d_6) δ 8.88(d, 6H), 7.96 (t, 6H), 7.30(d, 6H), 7.12 (t, 6H), 3.48 (s, 3H) ppm, ^{13}C NMR (100 MHz, DMSO-d_6 303 K) δ, 154.5, 152.2, 142.5, 137.4, 127.3, 121.6, 116.8 ppm, ^{195}Pt NMR -2103.5 ppm. Anal. Calcd. for $C_{33}H_{27}N_9Pt_3Cl_6$, C, 29.41, H, 2.02, N, 9.35, Found C, 29.63, H, 1.98, N, 9.10.

PtC5, Yield, 118 mg, (53 %). ^{1}H NMR (400 MHz, DMSO-d_6) δ 8.80(d, 6H), 7.96 (t, 6H), 7.30(d, 6H), 7.10 (t, 6H) ppm, ^{13}C NMR (100 MHz, DMSO-d_6) δ, 157.4, 154.8, 146.2, 137.2, 122.9, 120.8, 117.2 ppm, ^{195}Pt NMR -2104.2 and -2155.6 ppm. Anal. Calcd. for $C_{33}H_{24}N_{12}Pt_3Cl_6$, C, 28.59, H, 1.74, N, 12.12, Found C, 28.93, H, 1.54, N, 11.80; TOF MS ES$^+$, *m/z:* $[M\text{-}Cl]^+$ = 1351.0259.

Physical measurements

NMR spectra were recorded on a Bruker 400 MHz (1H) and a 100 MHz ((^{13}C) spectrometer. All chemical shifts are reported in δ (ppm). Elemental analyses were performed on Thermal Scientific Flash 2000 and mass spectra recorded on LCT Premier micro-mass Spectrometer. The Carbon shifts were recorded with reference to the relevant solvent signal while those of protons were referenced to tetramethylsilane ($Si(CH_3)_4$) while ^{195}Pt spectra were referenced to K_2PtCl_6 in D_2O. Kinetic studies for fast reactions were monitored using an Applied Photophysics SX20 stopped-flow spectrophotometer coupled to an online data acquisition system. A Varian Cary 100 Bio UV-Vis spectrophotometer thermostated by a Varian Peltier

temperature controller to within ±0.05 ^{o}C was used for the slow kinetic measurements. The kinetic traces were analyzed using the Origin 7.5® software package.[39] The pH of the solutions was recorded on a Jenway 4330 pH meter calibrated using standard buffer solutions of pH 4.0, 7.0 and 10.0.

Preparation of complex solutions

Owing to poor solubility of the chloro complexes they were converted to aqua analogues according to reported method.[40-44] Aqua solutions were prepared by refluxing chloro complexes with equivalent amount of silver perchlorate. Perchlorate salts are preferred due to their high solubility in water and are kinetically stable. The solutions were refluxed at 40-50 ^{o}C for 48 hours in 0.1 M $HClO_4$ (50 mL). Perchlorate salts and $HClO_4$ acid were used as inert electrolytes and ClO_4^- anion is non-complexing ion. It provides strong acidity with minimal interference since it is weakly nucleophilic. Increased acidity results from the conjugate base of $HClO_4$ acid, ClO_4^- anion that has its negative charge distributed equally over the four oxygen atoms. This delocalization of the conjugate base, ClO_4^- anion, contributes to the increased acidity of $HClO_4$ acid than HCl acid. Also $HClO_4$ acid is not susceptible to hydrolysis. As such $HClO_4$ acid and perchlorate salts were used to adjust ionic strength in kinetic studies where other electrolytes might complex the metal ion. The AgCl precipitate was removed by filtration through 0.45 µmilli-pore membrane filter. The removal of the Cl^- ions by Ag^+ to form $AgCl_{(s)}$ ensured presence of platinum aqua species, $[Pt(OH_2)_2]^{2+}$ in the solution and ClO_4^- as the counter ion.. This is supported by the pK_a values that indicate at pH 2.0 the major species involved in kinetics processes are aqua species. The resulting aqua solutions were titrated with NaOH solution to determine the pK_a values of the complexes for kinetic investigations.

pK_a determination of the aqua complexes

Spectrophotometric pH titrations were carried out on UV-Vis spectra on a Varian Cary 100 Bio spectrophotometer. NaOH was used as the base for spectrophotometric titration in the pH range 1 – 10. To avoid absorbance corrections due to dilution a large volume of the platinum aqua complex (250 mL) was used. To avoid leaching of chloride ions, 500 µL of the sample taken in ampoules were placed on the electrode and pH recorded then discarded. The pH was adjusted by adding 0.01, 0.05, 0.10 and 0.50 M solutions of either NaOH or $HClO_4$ acid. The pH of the

solution was maintained at pH 2.0 based on the pK_a study and the ionic strength was maintained at 0.1 M using $NaClO_4$.

Kinetic measurements

Spectral changes resulting from mixing the trinuclear Pt(II) complex and nucleophile solutions were recorded over the wavelength range 200 to 800 nm to establish a suitable wavelength at which kinetic measurements were performed. A summary of the used wavelength for each nucleophile is summarized in Table S1 (Electronic Supporting Information). All kinetic measurements were performed under *pseudo*-first-order conditions at least 20 fold and 60-fold excess of the nucleophile over that of the metal concentration for mononuclear and trinuclear complexes respectively. This ensured at least 10-fold of nucleophiles concentration at each platinum centre hence forced the reaction to completion. The temperature was controlled throughout all kinetic experiments within an accuracy of ±0.05 ^{o}C. Activation parameters ($\Delta H^{\#}$ and $\Delta S^{\#}$) were measured as a function of temperature over a temperature range of 15 to 40 ^{o}C at an interval of 5 ^{o}C. The reported rate constants represent an average value of at least six to eight independent kinetic runs for each set of experimental conditions on the stopped flow and a triplicate for UV-Visible spectrophotometer. All data obtained from both the UV-Visible and stopped flow spectrophotometric techniques were fitted to first-order exponential function to generate the pseudo-first-order rate constants (k_{obs}). The reactions were followed by the changes in absorbance at suitable wavelengths for both fast reactions on the stopped flow and slow ones on the UV-Vis spectrophotometer.

Computational Calculations

Density functional theory (DFT) calculations were performed with the Gaussian 09 package.[45] All these DFT calculations were performed using Becke's[46] three parameter exchange functional (B3) combined with both Lee- Yang-Parr gradient corrected correlation functional (LYP) using LanL2DZ as the basis set. B3LYP refers to a three parameter functional hybrid exchange of Becke with functional correlation gradient of Lee, Yang and Parr,[47] whereas LANL2DZ refers to Los Alamos National Laboratory 2 Double ζ basis set.[48] The study utilized the B3LYP/LANL2DZ level of theory in gas phase to model the structural and electronic properties of the complexes. The singlet states were used due to low electronic spin of Pt(II) complexes. To understand the electronic structures of the studied complexes, DFT calculations

were carried out. The ground-states electronic structures were calculated to enable determine the energies of molecular orbitals. The optimized structures and plots were created by Gauss View.[49] The optimized molecular structures are presented in Figure 1 while the labeling of the atoms is shown in Figure 2. The DFT-optimized structure of **PtC1** shows the dihedral and basal angles between two pyridyl groups chelated to Pt(II) centre. Selected bond lengths, bond angles and other parameters are given in Table 1.

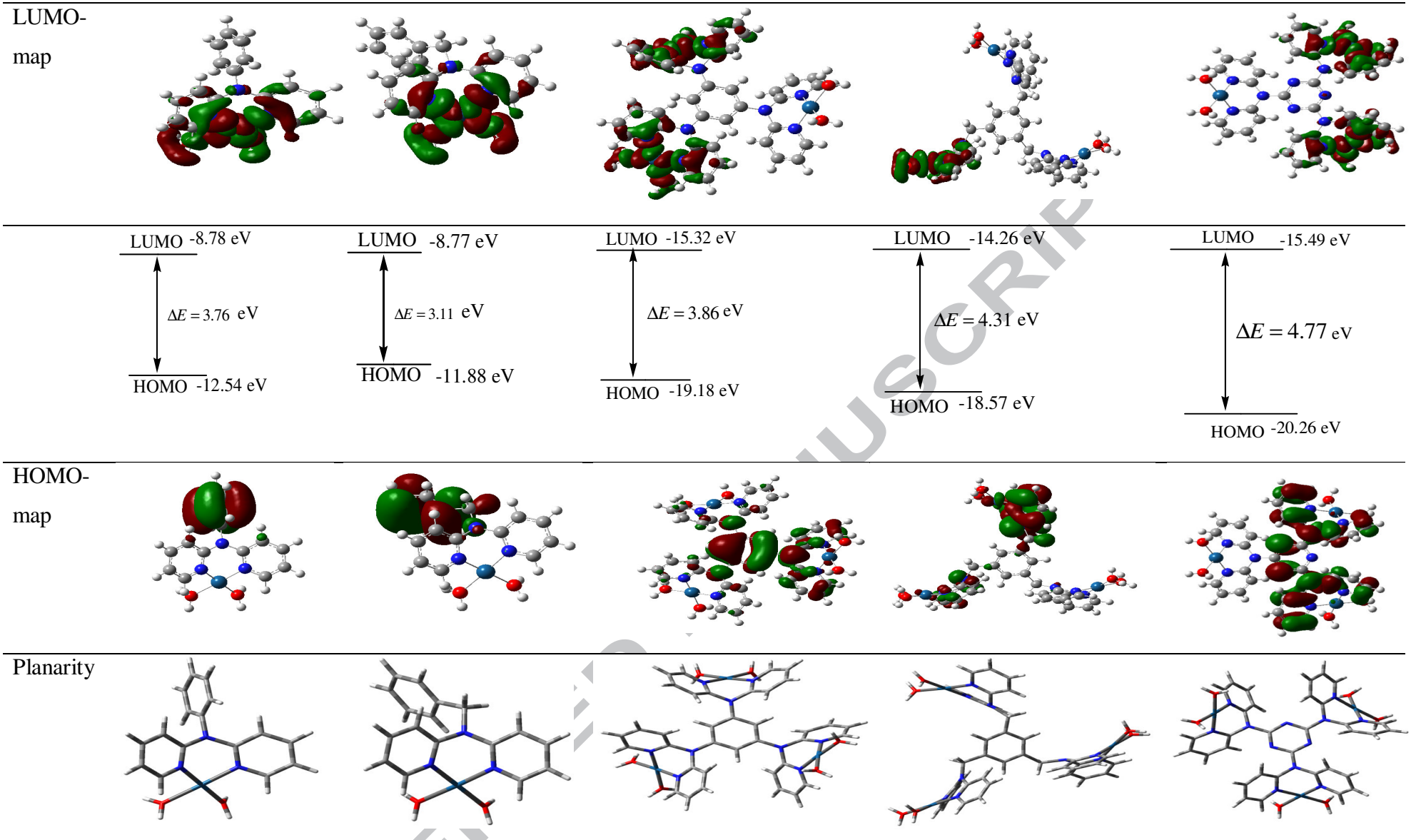

Figure 1: DFT optimized structures of HOMO and LUMO frontier molecular orbitals of the platinum(II) complexes at B3LYP/LANL2DZ level theory (Isovalue = 0.02).

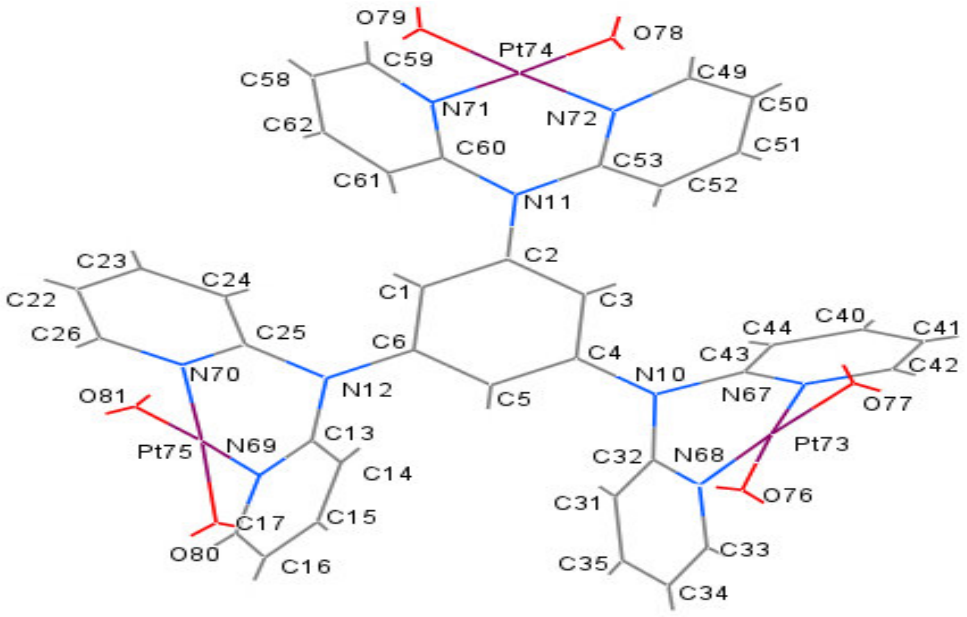

Figure 2: Optimized molecular structure of **PtC3** showing the coordination spheres of the complex. Hydrogen atoms were not labeled for clarity. Extracted data is summarized in Table 1.

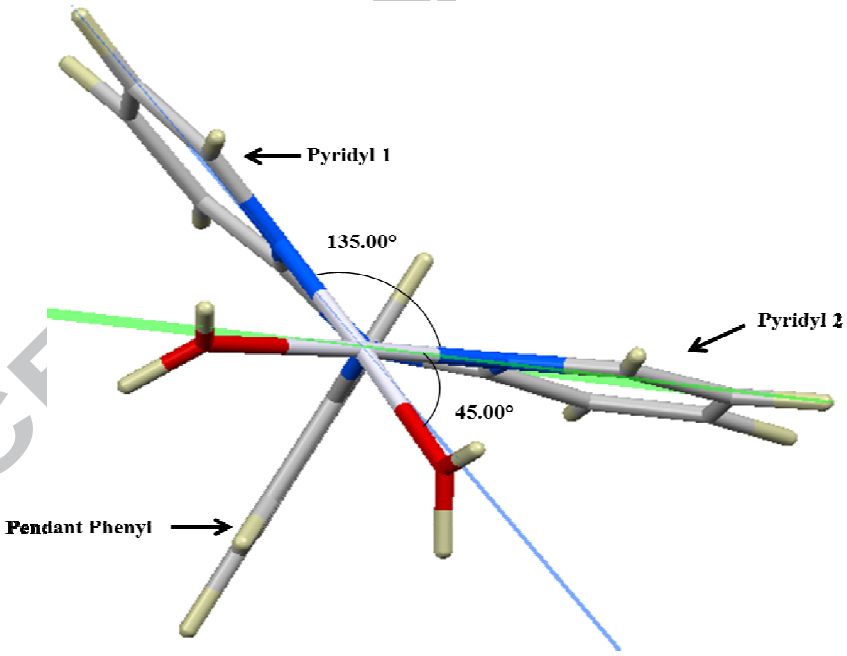

Figure 3: DFT-optimized structure of **PtC1** showing the dihedral and basal angle between two pyridyl groups. The dihedral and basal angles have minimal effect on the reactivity of the complexes.

Table 1: Selected bond lengths (Å), bond angles (degrees) and NBO charges for the various atoms of the complexes

Complex		**PtC1**	**PtC2**	**PtC3**	**PtC4**	**PtC5**
HOMO-LUMO ΔE						
LUMO/eV		-8.78	-8.77	-15.32	-14.26	-15.49
HOMO/eV		-12.54	-11.88	-19.18	-18.57	-20.26
ΔE/eV		3.76	3.11	3.86	4.31	4.77
Electrophilicity index (ω) (eV)		30.22	34.20	77.09	62.41	66.88
NBO Charges on: Pt		0.755	0.760	0.786	0.781	0.786
				0.786	0.772	0.786
				0.786	0.772	0.786
Dipole moment (Debye)		5.9126	6.4378	2.6377	4.6285	2.7545
Inter-atomic distance (Å)	C4-N10	1.4736	1.5128	1.4530	1.5026	1.4122
	C32-N10	1.4135	1.4112	1.4391	1.4195	1.4477
	C43-N10	1.4135	1.4091	1.4391	1.4199	1.4467
Intermetallic distance (Å)	Pt73-Pt74			9.0082	11.1296	8.7157
	Pt73-Pt75			9.8967	11.5317	9.7200
	Pt74-Pt75			9.8964	12.6557	9.7201
Dihedral angle between pyridyl rings (°)		45	50.37	55.84	40.23	54.49

Inter-atomic distance were obtained from Figure 2

Determination of pK_a values for the aqua complexes

The pK_a titration studies were carried out to ascertain the acidity of the complexes. The established pK_a values ensured that kinetic studies were carried out with complexes in their aqua form. The pK_a titrations showed all the complexes to exist in aqua species at pH 2.0. Basing on this pK_a titration data, reaction of aqua complexes were performed at pH 2.0 to ensure that the complexes exist as aqua species. A typical UV-Vis spectrum recorded during spectrophotometric titration of the six-aqua complex with NaOH is shown in Figure 4. The pK_a values were determined from Boltzmann Equation 1 by fitting a characteristic sigmoid curve and locating the inflection point using the Origin 7.5® program. The pK_a values of the deprotonated complexes are summarized in Table 2 while the proposed deprotonation mechanism is represented in equilibrium reaction in Scheme 2 for mononuclear analogue.

$$y = A_2 + (A_1 - A_2)/(1 + \exp(x - x_0)/\partial x) \quad [1]$$

where A_1 and A_2 are initial and final y values respectively, x_0 = centre, ∂x = width. The y value at x_0 is half way between the two limiting values A_1 and A_2. The y value changes drastically within a range of x variable. The width of this range is approximately ∂x.

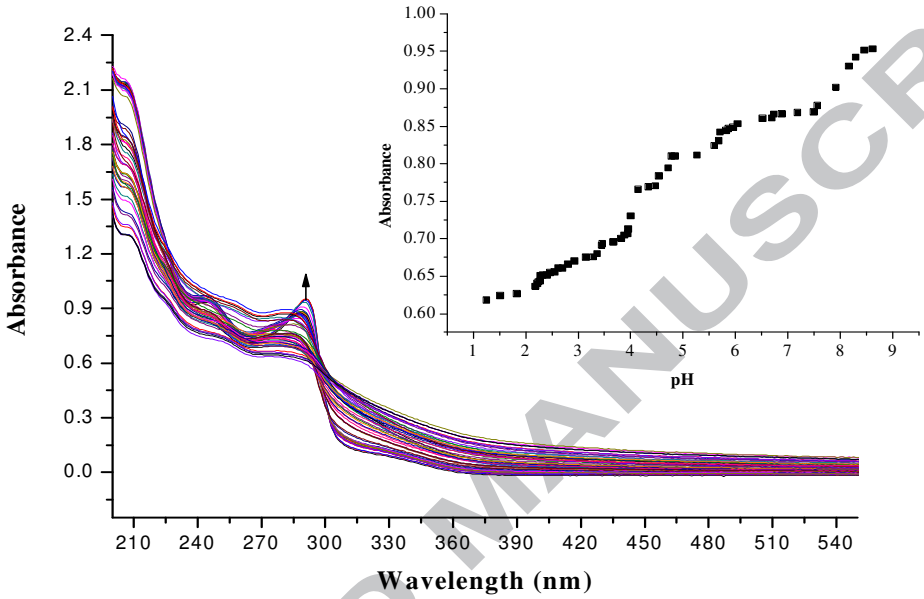

Figure 4: UV/Vis spectra for the titration of **PtC5** complex recorded as a function of pH in the range of 2 to 10 at 25 ^{o}C, *Inset* Plot of absorbance versus pH at λ = 295 nm.

Table 2: A summary of pK_a values obtained for stepwise deprotonation of aqua Pt(II) complexes investigated

Complex	PtC1	PtC2	PtC3	PtC4	PtC5
pKa_1	2.32 ± 0.01	2.87 ± 0.02	2.37 ± 0.08	2.53 ± 0.02	2.23 ± 0.02
pKa_2	4.53 ± 0.02	6.97 ± 0.11	3.30 ± 0.01	3.17 ± 0.01	3.34 ± 0.10
pKa_3			4.02 ± 0.01	3.60 ± 0.01	4.03 ± 0.02
pKa_4			4.78 ± 0.08	4.30 ± 0.01	4.66 ± 0.08
pK_{a5}			6.73 ± 0.07	5.42 ± 0.03	5.70 ± 0.04
pK_{a6}			8.45 ± 0.01	7.46 ±0.07	7.99 ± 0.03

The pK_a values are in the order **PtC5 > PtC1 > PtC3 > PtC4 > PtC2** which corroborates the electronic properties of the bridging ligands. The trend shows complexes with rigid linkers to have lower pK_a values compared to those with methylene groups. The reduced acidity of the complexes with flexible linkers is attributed to the inductive effect of methylene linker that

increases electron density on the dipyridyl rings.[49b] This makes deprotonation of the coordinated aqua ligands difficult due to increased electron density around the Pt(II) centre. The higher electron density in these compounds is supported by DFT calculations that show raised HOMO orbitals in complexes possessing methylene linkers. Raised HOMO orbitals signify addition of electrons to the respective orbitals. On the other hand, the low-lying LUMO orbitals in rigid complexes **PtC1**, **PtC3** and **PtC5** augment a better π-back-donation of electrons from the metal centre to the pendant phenyl ring. As mentioned earlier, back donation to the heterocyclic ligand (**PtC5**) stipulates the transfer of negative charge into its delocalized π-system i.e. the LUMO. The study shows the negative charge to be shared by more atoms in **PtC5** in Scheme 2 which is favourable for its reactivity. The low lying LUMO orbitals account for extensive delocalization in the complex. Electronic factors in rigid complexes are also exhibited by bond lengths of the atoms. For instance, the short C4-N10 in rigid complexes (1.4122 – 1.4736 Å) are indicative of partial double bond character (sp^2 hybridization) compared to methylene linked complexes with longer bond length (1.5026 – 1.5128 Å) indicating single bond character (sp^3 hybridization). This findings show more extended and effective delocalization in rigid complexes than flexible analogues. As such, higher acidity in rigid complexes is expected due to more effective π-back donation. This results are also in agreement with literature report[50a,51-53] showing methylene group to have inductive effect. The introduction of methylene spacers destroys the conjugacy of the complexes hence reduced acidity and reactivity.[54-56a]

The subsequent deprotonation values are higher due to lowering of overall charge of the complex. The decrease in charge in trinuclear complexes from 6^+ to 5^+ decreases the electrophilicity of the metal centres decreasing the acidity the complexes upon formation of hydroxo species. Thus, increase in pK_a trend reported is due to the decrease in the overall charge of the complexes. The higher pH values recorded for subsequent deprotonation was due to formation of the hydroxo species. Higher pH values are recorded due to hydroxo-aqua species in the solutions which are less reactive towards the entering ligands.

The introduction nitrogen atoms in the backbone of benzene (**PtC5**) lead to an increase in acidity of the coordinated aqua molecules. This is due to the π-accepting properties of triazine that reduce electron density from the metal centres. This increases electrophilicity of the metal

centres hence lower pK_a values. This is also supported by low lying HOMO orbitals that suggest removal of electrons from HOMO orbitals. Increased π-back bonding in **PtC5** is further supported by shorter C4-C10, C2-C11 and C6-N12 bond lengths (1.4122 Å) compared to N10-C32, N10-C43, N11-C53, N11-C60, N12-C13, N12-C25 (1.4477 Å). The variation in bond lengths in this complex indicates flow of electrons from 5*d* orbitals of the metal to the antibonding orbitals of triazine ring. Similar observation was also reported by Wang *et al.,*[38] and El-Ghayoury *et al*.[56b] Thus, the presence of hetero-atoms in the benzene ring enhances the transfer of negative charge into its π delocalized system that supports resonance as proposed in Scheme 2. The resonance property of the compound has a significant effect on both bond lengths and the acidity of the coordinated aqua ligands in this complex.[57] The conjugate base of this complex is proposed to enjoy resonance stabilization making it more acidic. This is reflected in the out-of ring nitrogen atoms showing sp^2 hybridization while the inner benzene nitrogen atoms possess high electron density due to increased π-back bonding in triazine backbone. Thus, the resonance effect on pK_a values in **PtC5** moiety agrees with predictable behaviour of the complex.

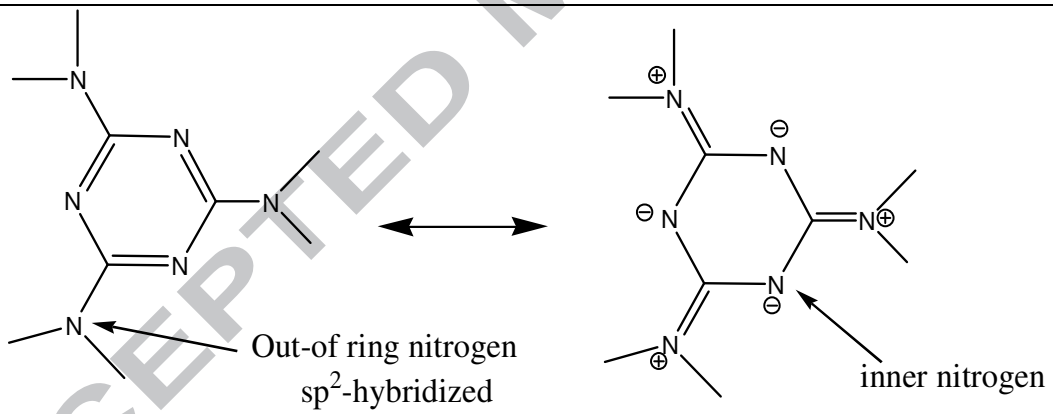

Scheme 2: The resonance hybrid structures of **PtC5** complex with 1,3,5-triazine backbone

Kinetic studies

The substitution reactions of coordinated aqua ligands with bio-relevant nucleophiles *viz.* **TU**, **DMTU** and **TMTU** was carried out under *pseudo*-first-order conditions using conventional UV-Visible spectrophotometry and stopped flow techniques. The suitable wavelengths for kinetics were determined by premixing equal volume of the complex with that of nucleophile in a tandem cuvette then mixing the solutions. A typical spectral change in a kinetic trace is shown Figure 5. The subsequent decrease in absorbance indicates the presence of two

subsequent reaction steps of **PtC5** with **TU**. The recorded kinetic traces were fitted to a single exponential function. Figure 6 shows typical plots of absorbance verses time for **PtC5** with **TU** and **DMTU** on the stopped flow while part (c) shows the kinetic trace with **TMTU** on the UV-Vis spectrophotometer.

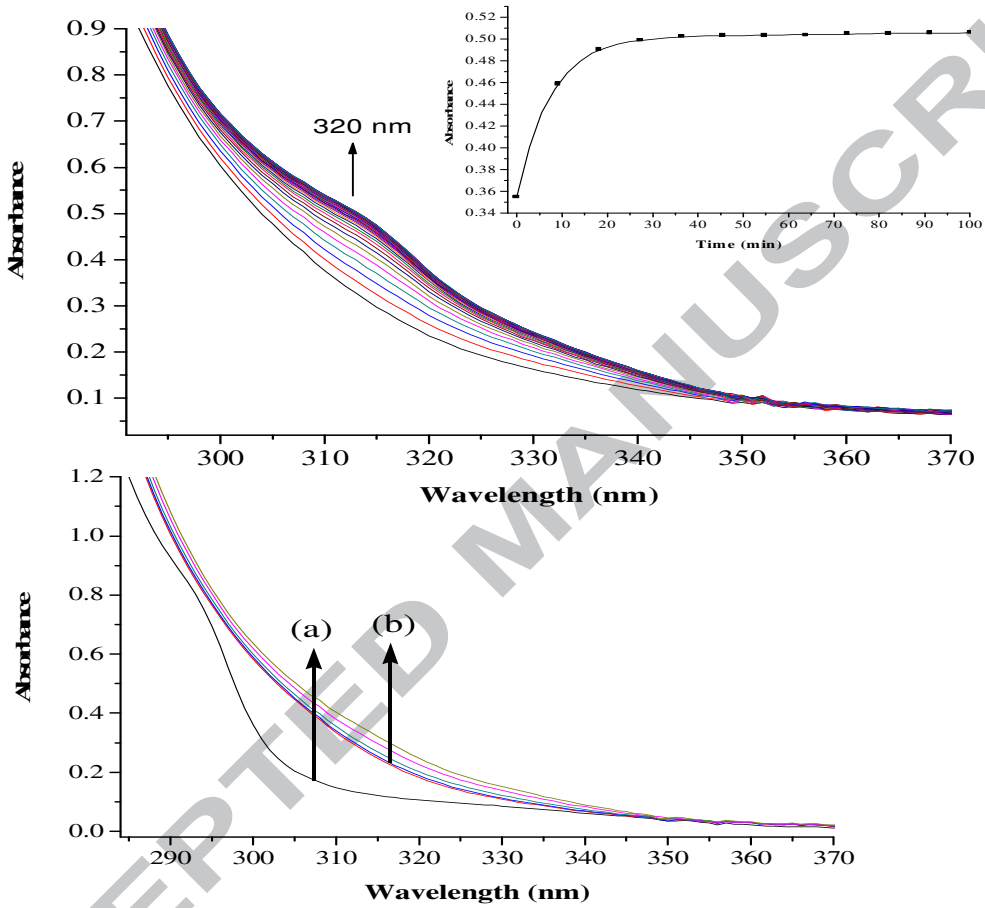

Figure 5: UV/Vis spectral changes during the reaction of **PtC5** and **TU** at T = 298.15 K, pH = 2.0 and I = 0.1 M $NaClO_4$. (a) Initial spectrum before adding **TU** and (b) spectrum at t = 30 s; successive spectra were recorded at an intervals of 5 min.

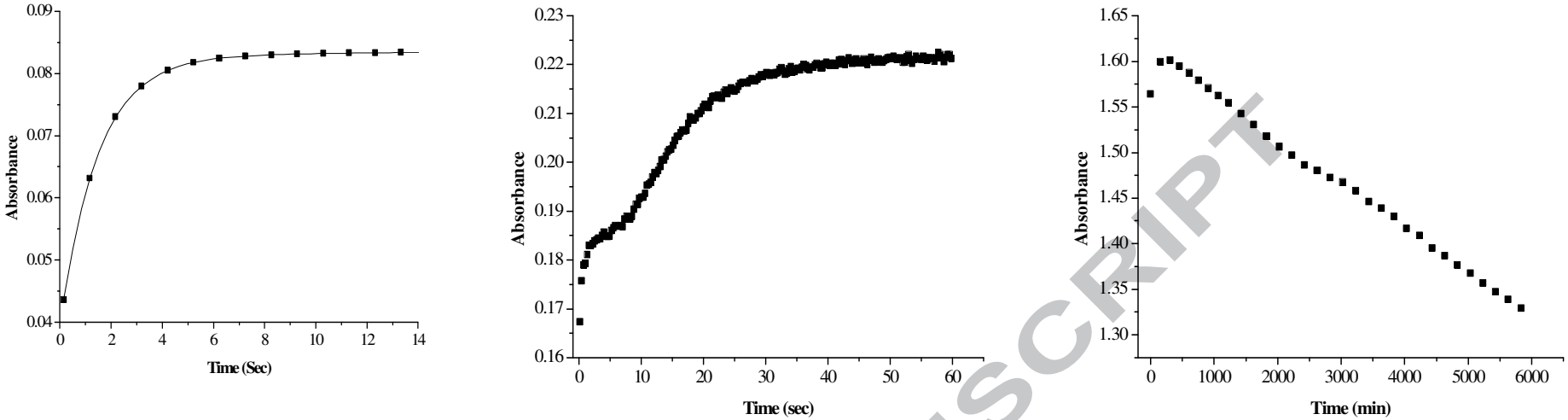

(a) **(b)** **(c)**

Figure 6: Typical kinetic traces showing a fast substitution reaction step of **PtC5** with (a) **TU** (b) **DMTU** on the stopped-flow while (c) is the last two steps of **TMTU** on UV-Vis spectrophotometer at T = 298.15 K, pH = 2.0, I = 0.1 M $NaClO_4$. The first step of **TMTU** was observed on the stopped-flow while the third step of **DMTU** was recorded on UV-Vis spectrophotometer.

The observed *pseudo*-first order constants, k_{obs} were obtained as average values of six to eight independent kinetic runs for each experimental condition on the stopped-flow and in triplicates on UV-visible spectrophotometry. The k_{obs} values were plotted against the entering nucleophile concentration. The plots are linear with zero or negligible intercept as shown in Figures 7, 8 and S3–S5 in the Electronic Supplementary Information. The rate constants (k_2) are linearly dependent on the concentration of entering of nucleophile. The $k_{obs(1,2,3)}$ is expressed by Equation [2].

$$k_{obs(1,2,3)} = k_{2(1st,\ 2nd,3rd)}[Nu] \qquad [2]$$

The second-order rate constants for reaction steps of the corresponding complexes at 25 ^{o}C are summarized in Table 3.

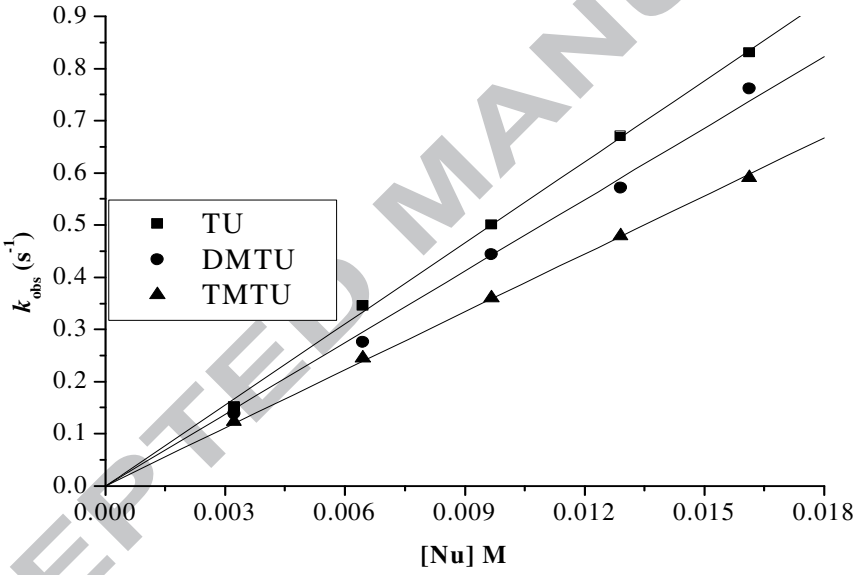

Figure 7: Plots of $k_{obs(1)}$ versus nucleophile concentration for the reaction of **PtC1** at pH = 2.0, T = 298.15 K, I = 0.1 M $NaClO_4$.

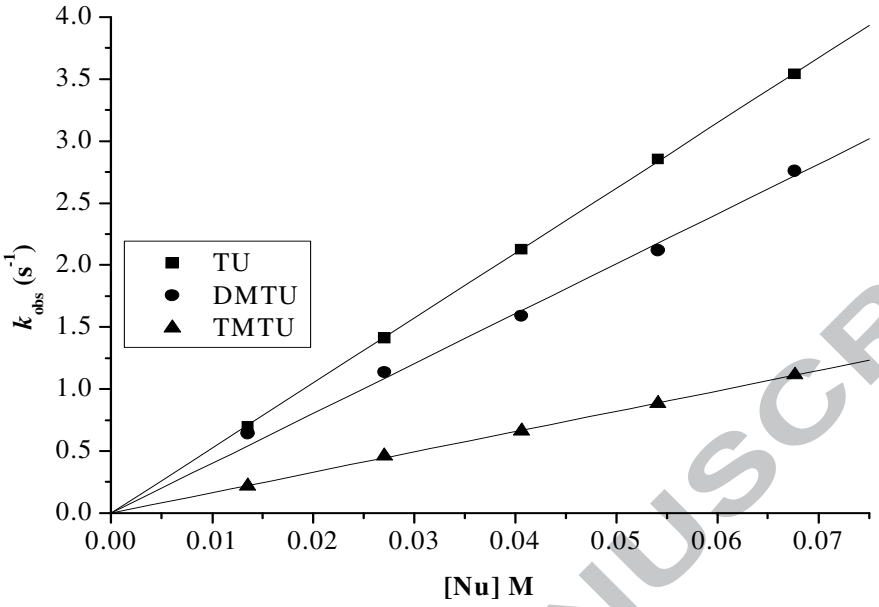

Figure 8: Plots of $k_{obs(1)}$ versus nucleophile concentration for the reaction of **PtC5** at pH = 2.0, T = 298.15 K, I = 0.1 M $NaClO_4$.

Table 3: A summary of the second order rate constants, k_2, for the reaction of the investigated complexes at pH = 2.0, T = 298.15 K and at I = 0.1 M $NaClO_4$

Complex	Nu	2nd order rate constant/$M^{-1}s^{-1}$		
		$k_{2(1st)}$	$k_{2(2nd)}$ x10^{-2}	$k_{2(3rd)}$ x10^{-3}
PtC1	**TU**	51.78 ± 0.40	4 ± 0.30	-
	DMTU	45.74 ± 0.77	1 ± 0.02	-
	TMTU	37.06 ± 0.22	-	-
PtC2	**TU**	33.34 ± 0.27	3 ± 0.40	-
	DMTU	25.09 ± 0.19	1 ± 0.01	-
	TMTU	11.45 ± 0.04	1 ± 0.02	-
PtC3	**TU**	40.71 ± 0.22	5 ± 0.30	
	DMTU	37.23 ± 0.55	1 ± 0.01	
	TMTU	15.64 ± 0.26	-	-
PtC4	**TU**	27.87 ± 0.25	6 ± 0.40	-
	DMTU	20.84 ± 0.14	2 ± 0.04	-
	TMTU	6.73 ± 0.05	0.5 ± 0.01	-
PtC5	**TU**	52.41 ± 0.11	4 ± 0.10	-
	DMTU	40.21 ± 0.68	64 ± 0.30	4 ± 0.1
	TMTU	16.43 ± 0.09	7 ± 0.10	Too slow

Activation parameters

To investigate thermodynamic and chemical stability of the complexes, reactivity was performed at various temperatures (15 °C to 40 °C. This enabled examine the changes in thermodynamic stability *viz* the enthalpy, $(\Delta H^{\#})$ and the entropy, $(\Delta S^{\#})$ of activation. These activation parameters were determined from the Eyring plots illustrated in Figures 9 and 10 and (S6-S8) using Equation 3. The complexes showed kinetic stability at all temperatures that conferred thermostability of the investigated class of Pt(II) complexes.

$$In\left(\frac{k_2}{T}\right) = -\frac{\Delta H^{\#}}{RT} + \left[In\left(\frac{k_B}{h}\right)\right] + \frac{\Delta S^{\#}}{R} = \frac{\Delta H^{\#}}{RT} + \left(23.8 + \frac{\Delta S^{\#}}{R}\right) \quad [3]$$

where k_B and h are Boltzmann's and Planck's constants respectively while R is gas constant and T is absolute temperature.

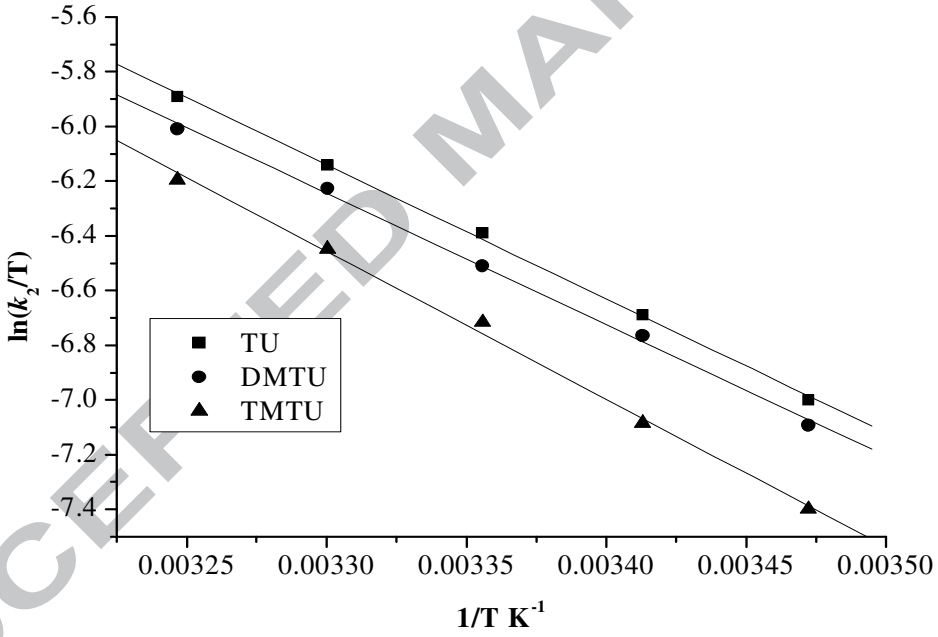

Figure 9: Eyring plots for first substitution step of **PtC1** monitored on stopped-flow spectrophotometer at I = 0.1 M $NaClO_4$, pH = 2.

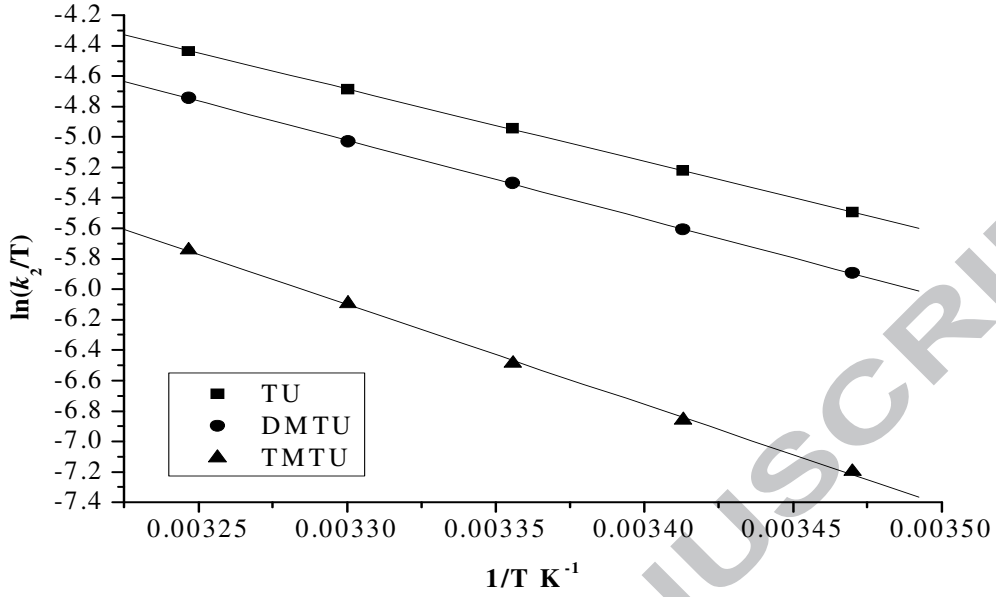

Figure 10: Eyring plots for the first substitution step of **PtC5** monitored on stopped-flow spectrophotometer at I = 0.1 M $NaClO_4$, pH = 2.0.

Table 4: A summary of the activation parameters for the substitution of aqua ligands pH = 2.0 and at I = 0.1 M $NaClO_4$

Complex	Nu	Activation Enthalpy/ kjmol^{-1}		Activation entropy/ J mol^{-1}K^{-1}	
		$\Delta H_1^{\#}$	$\Delta S_1^{\#}$	$\Delta H_2^{\#}$	$\Delta S_2^{\#}$
PtC1	**TU**	40.83 ± 0.9	-114 ± 3	21.91 ± 0.4	-229 ± 1
	DMTU	39.97 ± 1.2	-118 ± 4	29.89 ± 0.4	-213 ± 1
	TMTU	44.93 ± 1.5	-103 ± 5	-	-
PtC2	**TU**	39.81 ± 0.3	-121 ± 1	20.54 ± 0.8	-249 ± 2
	DMTU	43.47 ± 1.7	-111 ± 6	26.74 ± 0.9	-241 ± 3
	TMTU	40.86 ± 0.8	-126 ± 3	41.02 ± 1.5	-179 ± 5
PtC3	**TU**	39.58 ± 0.8	-108 ± 3	28.20 ± 1.0	-209 ± 3
	DMTU	40.48 ± 0.7	-106 ± 2	33.33 ± 0.8	-200 ± 3
	TMTU	53.30 ± 1.2	-66 ± 4	-	-
PtC4	**TU**	38.60 ± 0.9	-116 ± 3	23.31 ± 0.3	-221 ± 1
	DMTU	30.00 ± 0.5	146 ± 2	30.41 ± 0.6	-204 ± 2
	TMTU	45.22 ± 1.1	-104 ± 4	44.48 ± 0.1	-164 ± 1
PtC5	**TU**	39.49 ± 0.3	-107 ± 1	32.80 ± 0.4	-194 ± 1
	DMTU	44.04 ± 1.4	-94 ± 5	30.80 ± 0.5	-165 ± 2
	TMTU	52.10 ± 0.8	-74 ± 3	51.09 ± 1.3	-121 ± 4

The small positive enthalpies and significantly large negative entropy values support an associative mode of substitution mechanism commonly reported for the Pt(II) square-planar complexes.[58-61] In this mode of mechanism, the ML_3X complex binds to the incoming ligand Y to form a five-coordinate intermediates $(ML_3XY)^{\#}$ as shown in Scheme 3. Substitution of X results in a 16 electron complex ML_3Y in which the negative activation entropy indicates an increase in the order of the transition state relative to the reactants.[58,59] The small positive enthalpy values reported in Table 4 is attributed to bond formation before bond breaking in the transition state.[60,61]

Substitution reaction

Since it is unlikely for the entering nucleophile to displacement six water molecules by a single kinetic phase, a biphasic reaction is proposed at each metal centre. The first step is attributed to fast substitution of one water molecule at each metal centre. The second phase is composed of two simultaneous reactions; where the second water molecule is displaced followed by a dechelation process. The extent of the second step was governed by the steric hindrance caused by coordination of the first nucleophile. The much slower second step was joined by the displacement of the labilized linker due to the strong *trans* effect of thiourea coordination. The

proposed reaction mechanism with thiourea as the entering nucleophile is shown in Scheme 3. This shows S-donor ligands as strong and efficient nucleophile that can compete with DNA for binding to Pt(II) complexes.

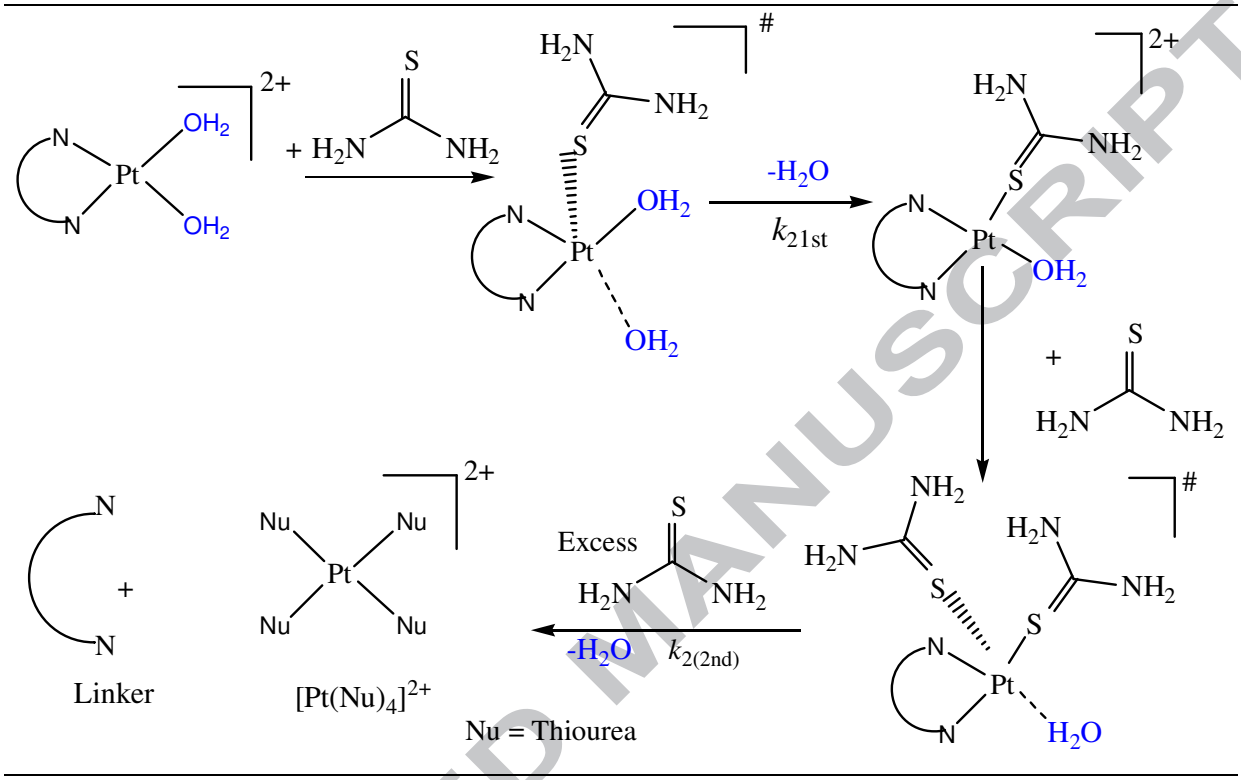

Scheme 3: Proposed substitution mechanism showing biphasic substitution at each Pt(II) centre followed by the dechelation process

The dechelation step was confirmed using ^{1}H and ^{195}Pt NMR kinetics by monitoring coordination details of the reactants and products (Figures 11 and 12). Coordination of the ligand to the metal ion causes ^{1}H chemical shifts. Figure 11 shows an array of ^{1}H NMR spectra for the reaction between **PtC3** with 6 equivalents of thiourea. The spectra show net chemical shifts of the coordinated pyridyl protons indicating changes in their coordination environment. The dipyridyl protons denoted $\mathbf{H_a}$ were monitored due their proximity to *N*-donor atoms when coordinated to the metal centre. Their resonance on the chloro complex appear downfield at δ = 8.88 ppm that indicates coordination of platinum atom. This downfield shift is due to the change in electron density on coordination to the metal atom. On reaction with excess **TU** the $\mathbf{H_a}$ protons shift to $\mathbf{H_a}$', which appear upfield at δ = 8.28 ppm similar to those of uncoordinated

ligand. A decrease in electron density on the pyridyl by the σ effect yields to this downfield shift at all ring positions on complexation.

A signal peak shown at δ = -2103.5 ppm by ^{195}Pt NMR is consistent with platinum(II) complexes with *cis*-PtN_2Cl_2 configuration.[62,63] On reaction with 6 equivalents of **TU** shows a peak at -3905.6 ppm with no reaction intermediates (Figure 12). This shifting of the peak indicates the preference of Pt(II) to coordinate to sulphur-donor ligands. The study show Pt-N adducts to be converted to Pt-S adducts.[64] The peak at -3906.6 ppm on ^{195}Pt NMR denotes formation of Pt(**TU**)$_4^{2+}$ complex when reacted with excess thiourea.[65,66] From experimental data both the ^{1}H and ^{195}Pt NMR support the complexes to undergo displacement of the linker induced by strong *trans* effect of the sulphur donor atoms.[67]

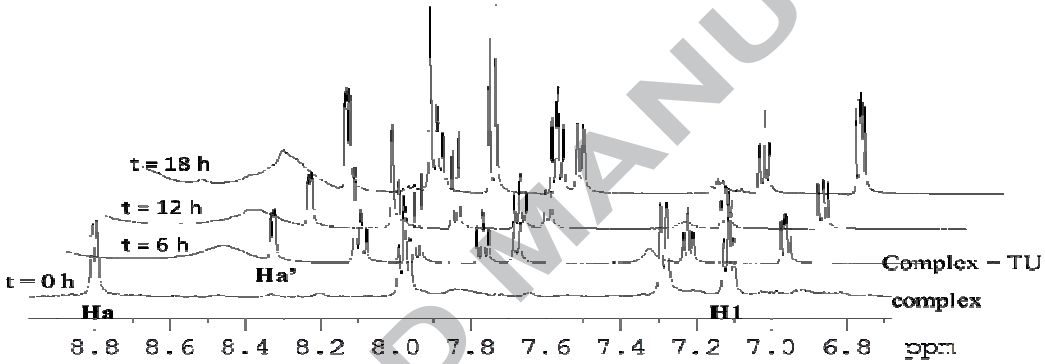

Figure 11: Time dependent stacked plot of ^{1}H NMR spectra of **PtC3** with 6 equivalents of TU undergoing dechelation to liberate the bridging linker.

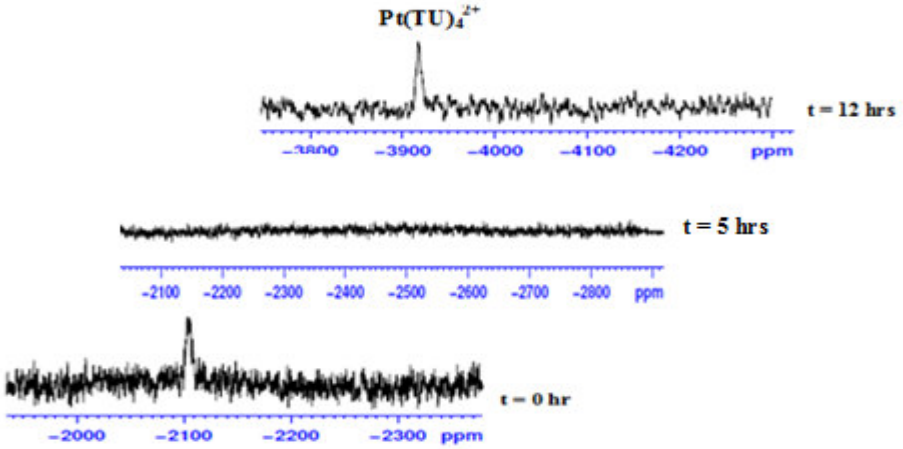

Figure 12: Time dependent ^{195}Pt NMR shifts of **PtC3** in DMF forms [Pt(**TU**)$_4^{2+}$] on reaction with excess **TU**.

Discussion

This work reports on the reactivity of mono and trinuclear dipyridylamine Pt(II) complexes with biologically relevant molecules. With a view of shedding light on the role of rigidity verses flexibility of bridging moieties, the study shows that introducing methylene groups in the backbone of a complex significantly reduces its reactivity. However, the effect is opposite when a hetero atom or rigidity is introduced as the two enhances reactivity. The experimental results verifies this by showing a reactivity trend of **PtC5 > PtC1 > PtC3 > PtC2 > PtC4** with **TU** as the entering nucleophile. The trend is governed by both steric and electronic effects arising from the methylene spacers and heteroatoms in the backbone of the ligands. The high reactivity of **PtC5** is due to the decrease of electron density at the Pt(II) centre caused by enhanced π-back-donation *to* π^* orbitals of triazine ligand. The stronger π-acceptor of triazine stabilizes transition state by accepting electron density that is donated by the entering nucleophile to the metal centre. This increases electrophilicity at the Pt(II) centres that leads to high reactivity which is reflected in its lower pK_a values of the coordinated water ligands. This is caused by the presence of electronegative nitrogen atoms which leads to greater π-back-donation from metal centre to the triazine ring. On the other hand, complexes with flexible ligands (**PtC2** and **PtC4)** show slower reactivity than with rigid spacers (**PtC1** and **PtC3**). The study suggests methylene groups to increase electron density on the pyridyl rings and prevent effective π-back bonding.[68] Also the presence of lone pair electrons on the amine nitrogen makes them stronger σ donors than rigid counterparts. Thus, a combination of rigidity and delocalization accounts for the enhanced reactivity of rigid appended complexes. Rigidity and flexibility is proposed to have a significant influence on the reactivity of the complexes.

The high reactivity of **PtC5** is also attributed to the increase in the number of ring electrons when =CH- are replaced by nitrogen atoms. Each nitrogen atom introduces two additional electrons making triazine ring to have six non-bonding electrons in addition to its π-electrons. This unshared pair of electrons to some extent is delocalized and become part of the aromatic π-electron system in both ground and excited states.[69] This complex shows high π accepting property but decreased σ-donor strength as electronegativity is within the ring is increased. This leads to delocalization of the $d\pi$ electrons from the metal to the empty π^* orbitals of the triazine ring. The electron withdrawing effect of 1,3,5-triazine cycle is supported by the lowered HOMO orbitals and wider HOMO-LUMO gap (ΔE = 4.77 eV) Table 1. The

withdrawal of electron density lowers and stabilizes the HOMO orbitals. This is also reinforced by the presence of low-lying LUMO orbitals which increases π-back-bonding. It should also be noted that in **PtC3**, the amino nitrogen lone pair does not favour conjugation with the central benzene ring due to steric interactions with *ortho* hydrogen atoms. Hence there is reduced π-back donation compared to **PtC5**. In **PtC5** the amino nitrogen lone pair conjugates with triazine ring due to absence of *ortho* hydrogen atoms.

Two consecutive steps were observed for trinuclear complexes **PtC3** and **PtC4** which supports the notion that the three platinum centres are in the same chemical environment. In contrast, **PtC5** shows more reaction steps with sterically hindered nucleophiles supporting the likelihood of fluxionality of the complex in solution.[70,71] The complex is reported to undergo dynamic interchange of chemically inequivalent groups.[71,71] The rotations and unsymmetrical nature of **PtC5** in solution presents the possibility of chemically distinct metal centres as shown in Figure 13. However, this behaviour was not observed in **PtC3**. The ^{195}Pt NMR shows a single peak (Figure 12) that corresponds to one set of dipyridyl unit coordinated to Pt centre from the central benzene. This supports the previous study of **PtC3** to have symmetric structure in solution with all the three dipyridyl units in the same chemical environment.[38] Similarly, **PtC4** showed a single ^{195}Pt NMR spectrum at -2190.3 ppm. This value is consistent with N_2-$PtCl_2$ environment. Single peaks in **PtC3** and **PtC4** supports the number of substitution steps suggesting all the three metal atoms to be chemically equivalent.

In **PtC5** an increase in π electrons makes the complex to have a fluxional behaviour. This fluxionality favours the "up and down" structure that keeps the platinum centres in chemically different environment contrary to the expected symmetry of C_3 conformation. The "up and down" structure, is as a result of the axial and equatorial pyridyl groups undergoing interconversion through dynamic process in which the ring undergoes chair conformational change. This makes the electronic structure of **PtC5** to be different from **PtC3** that accounts for the difference in the kinetic and chemical shifts in **PtC5**.[72] The two peaks at -2104.2 ppm and -2156.6 ppm in the ratio of 2:1 by ^{195}Pt NMR spectra indicates platinum centres to be a chemically different environment. Based on this observation different number of substitution steps is expected from fluxional behaviour of **PtC5**.

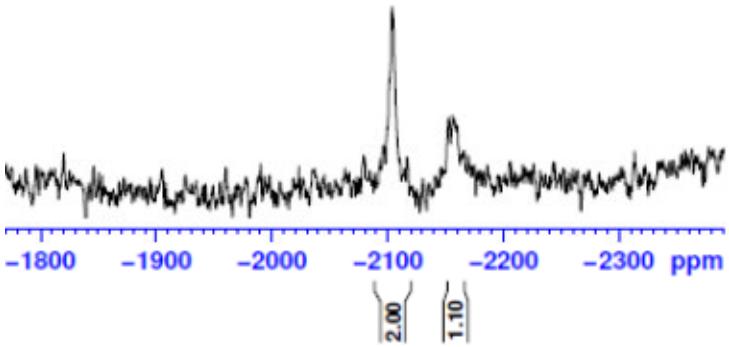

Figure 13: ^{195}Pt NMR spectra of complex **PtC5** in DMSO-d_6, showing presence of two inequivalent Pt(II) peaks

On reaction of **PtC5** with 6 equivalents of **TU**, the two peaks disappears signifying two independent platinum peaks. The study suggests the difference in the kinetic behaviour of trinuclear complexes to be influenced by the degree of conjugation of the amino nitrogen lone pair of electrons of the dipyridylamine unit with the central aromatic ring. The rates of reactions were dependent on the nature of entering nucleophile governed by steric effects in the order: **TMTU < DMTU < TU**.[65,73]

Conclusion

This study has illustrated that the nature of bridge between the metal centre and the pendant ligand has a significant influence the reactivity of the complexes. It shows that conformational rigidity enhances reactivity while incorporation of methylene groups retards reactivity. The acceleration in the reactivity in rigid complexes is attributed to the effective π-bonding between the metal centre and the pendant rings. On the contrary, introduction of methylene groups prevents such effective π-back bonding and increases electron density that results in a slower nucleophilic substitutions. The study further shows that replacement of –CH groups with N in the phenyl ring accelerates reactivity. Thus, the study shows that the π-accepting property of triazine ring increases the electrophilicity on the Pt(II) metal centre which increases nucleophilic substitution. The Low positive values of enthalpy of activation and significantly large negative values of entropy of activation parameters indicate an associative mechanism of substitution. The successful application of ligand substitution in multinuclear Pt(II) complexes marks the first step to development of new polynuclear antitumour agents. The route to novel anticancer drugs is based on mechanistic knowledge. Mechanistic knowledge on reactions of

these multinuclear Pt(II) complexes under biological and physiological conditions remains the basis for development of these novel antitumour drugs. Such inventions and explorations will most likely provide an alternative to modern cancer treatment. After successful substitution reactions of these complexes, further research will explore how these compounds bind to DNA molecule at physiological pH and physiological concentrations. Further investigation will test the complexes in cancer cell lines and *in vivo*.

Acknowledgements

The author thanks the University of Kwazulu Natal for the doctoral scholarship to carry out this research. The financial support to PA is greatly appreciated. The author thanks Dr Allen Mambanda for his suggestions towards the writing of this paper. I am also grateful to Mr. Craig Grimmer and Miss Janse van Resenburg for characterization of the complexes.

Electronic Supplementary Information (ESI†) Available:

Selected wavelengths used for kinetic measurements, Tables of observed *pseudo*-first-order rate constants, Eyring plots, Mass spectrometry: the mass spectral data showing respective molecular ions and their fragmentation pattern, NMR data for ^{1}H NMR ^{13}C NMR and ^{195}Pt NMR, pK_a titration spectra of the complexes.

References

1. W. Yanqing, W. Xiaoyong, W. Jing, Z. Yongmei, H. Weijiang and G. Zijian, *Inorg. Chem.*, 2011, **50**, 12661-12668.
2. I. Ali, W. A. Wani, K. Saleem and A. Haque, *Anti-Cancer Agents in Medicinal Chemistry*, 2013, **13**, 296-306.
3. L. Ronconi, A. M. Pizarro, R. J. McQuitty and P. J. Sadler, *Chem. Eur. J.*, 2011, **17**, 12051-12058.
4. A. M. Florea and D. Büsselberg, *Cancers.*, 2011, **3**, 1351-1371.
5. N. J. Wheate and J. G. Collins, *Curr. Med. Chem.-Anti-Cancer Agents*, 2005, **5**, 267-279.
6. Y. M. Zhao, J. W. He, P. F. Shi, J. H. Zhu, L. Qiu, L. P. Lin and Z. J. Guo, *Dalton Trans.* 2006, 2617–2619.
7. N. J. Wheate and J. G. Collins, *Coord. Chem. Rev.*, 2003, **241**, 133-145
8. M. Frezza, S. Hindo, D. Chen, A. Davenport, S. Schmitt, D. Tomco and Q. P. Dou, *Curr. Pharm. Des.*, 2010, **16**, 1813-1825.
9. X. Y. Wang and J. Z. Guo, *Dalton Trans.,* 2008, 1521–1532.
10. N. J. Wheate, S. Walker, G. E. Craig and R. Oun, *Dalton Trans.*, 2010, **39,** 8113- 8127.
11. S. A. Adnan and Mika K, *Curr. Med. Chem.*, 2006, **13**, 1337-1357.
12. Wang X. Y, *Anti-Cancer Agents Med. Chem.,* 2010, **10**, 396–411.
13. J. B. Mangrum and N. Farrell, *J. Chem. Soc. Chem. Comm.*, 2010, **46**, 6640-6650.
14. D. M. Fan, X. L. Yang, X. Y. Wang, S. C. Zhang, J. F. Mao, J. Ding, L. P. Lin, Z. J. Guo, *J. Biol. Inorg. Chem.* 2007, **12**, 655–665.
15. M. X. Lin, X. Y. Wang, J. H. Zhu, D. M. Fan, Y. M. Zhang, J. F. Zhang and Z. J. Guo, *Apoptosis,* 2011, **16**, 288–300.
16. J. D. Roberts, J. Petroutka and N. Farrell, *J. Inorg. Biochem.*, 1999, **77**, 51-57
17. X. Wang and Z. Guo, *Chem. Soc. Rev.*, 2013, **42**, 202-224.
18. R. A. Ruhayel, J. S. Langner, M. J. Oke, J. Susan, S. J. Berners-Price, I. Zgani and N. Farrell, *J. Am. Chem. Soc.*, 2012, **134**, 7135-7146.
19. Z. Yongmei, H. Weijiang, S. Pengfei, Z. Jianhui, Q. Lin, L. Lipng and G. Zijian, *Dalton Trans.*, 2006, 2617-2619.

20. J. H. Zhu, Y. M. Zhao, Y. Y. Zhu, Z. Y. Wu, M. X. Lin, W. J. He, Y. Wang, G. J. Chen, L. Dong, J. F. Zhang, Y. Lu and Z. J. Guo, *Chem.-Eur. J.,* 2009, **15**, 5245–5253.
21. G. J. Kumar, H. V. S. S. Bomma, E. Srihari, S. Shrivastava, V. G. M. Naidu, K. Srinivas and V. J. Rao, *Med. Chem. Res*., 2013, **22**, 5973-5981.
22. L. Ronconi and P. J. Sadler, *Coord. Chem. Rev*., 2007, **251**, 1633-1648.
23. M. J. Rauterkus, S. Fakih, C. Mock, I. Pascasu and B. Krebs, *Inorg. Chim, Acta*., 2003, **350**, 355-365.
24. I. Puscasu, C. Mock, M. J. Rauterkus, A. Röndigs, G. Tallen, S. B. Gangopadhyay, J. E. A. Wolff and B. Krebs, *Z. Anorg. Allg. Chem*., 2001, **627**, 1292-1298.
25. M. J. Bloemink, H. Engelking, S. Karentzopoulos, B. Krebs and J. Reedijk, *Inorg. Chem*., 1996, **35**, 619-627
26. R. B. Weiss and M. C. Christian, *Drugs*, 1993, **46**, 360-377
27. J. Bogojeski and Ž. D. Bugarčić, *Trans. Met. Chem*., 2011, **36**, 73-78.
28. M. V. Beusichem and N. Farrell, *Inorg. Chem*., 1992, **31**, 634-639.
29. J. Reedijk, *Chem. Rev.,* 1999, **99**, 2499-2510.
30. W. E. Curtis, M. E. Muldrow, N. B. Parker, R. Barkley, S. L. Linas and J. E. Repine, *Proc. Natl. Acad. Sci.* USA, 1988, **85**, 3422-3425.
31. A. P. Wangoli and D. Jaganyi, *DOI 10.1002/kin.21085*, © 2017 Wiley Periodicals, *Inc. Int J Chem Kinet* 1–17, 2017.
32. A. Bianca, D. J. Bray, J. K. Clegg, K. Gloe, G. Karsten, O. Kataeva, F. L. Lindoy, J. C. McMurtrie, P. J. Steel, C. J. Sumby and M. Wenzel*, Dalton Trans.*, 2006, 4783-4794.
33. C. Tu, J. Lin, Y. Shao and Z. Guo, *Inorg. Chem.*, 2003, **42**, 5795-5797.
34. J. Pang, Y. Tao, S. Freiberg, Y. Xiao-Ping, M. D'Iorio and S. Wang, *J. Mater. Chem*., 2002, **12**, 206-212.
35. N. Wannarit, O. Roubeau, S. Youngme and P. Gamez, *Eur. J. Inorg. Chem*., 2013, 730-737.
36. S. Fakih, W. C. Tung, D. Eierhoff, C. Mock, and B. Krebs, *Z. Anorg. Allg. Chem.*, 2005, **631**, 1397-1402.
37. S. Corey, J. Pang and S. Wang, *Eur. J. Inorg. Chem*., 2002, 1390-1399.

38. Q. De Liu, W. Jia, G. Wu and S. Wang, *Organometallics*, 2003, **22**, 3781–3791.
39. V.B. Origin7.5^{TM} SRO in Origin Lab Corporation, Northampton, One, Northampton, MA, 01060, USA, 2003.
40. J. Bogojeski, Ž. D. Bugarčić, R. Puchta and R. van Eldik, *Eur. J. Inorg. Chem.,* 2010, 5439-5445.
41. S. Jovanović, B. Petrović, D. Čanović and Ž. D. Bugarčić, *Int. J. Chem. Kinet*., 2011, **43**, 99-106.
42. N. Hochreuther, S. T. Nandibewoor, R. Puchta, R. van Eldik, *Dalton Trans*., 2012, **41**, 512-522.
43. T. Soldatović, Ž. D. Bugarčić and R. van Eldik, *Dalton Trans*., 2009, 4526-4532.
44. N. Summa, R. Schiessl, N. Puchta, H. van Eikema and R. van Eldik R, *Inorg. Chem*., 2006, **45**, 2948-2958.
45. M. J. Frisch *et al*., Gaussian 09, Revision A.1, Gaussian, Inc. Wallingford CT, 2009.
46. a) A. D. Becke *J. Chem. Phys.* 1993, **98**, 1372-1377, 5648. (b) P. J. Stephens, F. J. Devlin, C. F. Chabalowski and M. J. Frisch, *J. Phys. Chem*. 1994, **98** 1623-1627.
47. (a) B. Miehlich, A. Savin, H. Stoll and H. Preuss, *Chem. Phys. Lett.*, 1989, **157**, 200-206; (b) P. J. Hay and W. R. Wadt, *J. Chem.Phys.,* 1985, **82**, 299-310.
48. C. Lee, W. Yang, R. G. Parr, *Phys. Rev. B.,* 1988, **37**, 785-789.
49. (a) A. Frisch, H. P. Hratchian, R. Dennington, T. A. Keith and J. Millan, Gauss View Version 5, Semichem Inc. KS, 2009. 5-15. (b) P. Wang, R. Humphry-Baker, J. E. Moser, S. M. Zakeeruddin and M. Grätzel, *Chem. Mater*., 2004, **16**, 3246-3251.
50. (a) D. Jaganyi, A. Hofmann and van R. Eldik, *Angew. Chem. Int. Ed.,* 2001, **40**, 1680-1683; (b) N. Hochreuther, R. Puchta, R. van Eldik, *Inorg. Chem*., 2011, **50**, 8984-8996.
51. J. Tournon and M. A. El-Bayoumi, *J. Am. Chem. Soc*., 1971, **93**, 6396-6398.
52. R. Tandon, T. A Nigst and H. Zipse, *Eur. J. Org. Chem*., 2013, 5423-5430.
53. H. Ertürk, A. Hofmann, R. Puchta and R. van Eldik, *Dalton Trans.,* 2007, 2295-2301
54. F. G. Bordwell and G. J. McCollumn, *J. Org. Chem*., 1976**, 41**, 2391-2395.
55. K. B. Wiberg, J. Ochterski and A. Streitwieser, *J. Am. Chem. Soc*., 1996, **118**, 8291-8299.

56. (a) P. C. Hiberty and C. P. Byrman, *J. Am. Chem. Soc*., 1995, **117**, 9875-9880. (b) D. G. Branzea, A. Fihey, T. Cauchy, A. El-Ghayoury, and N. Avarvari, *Inorg. Chem.*, 2012, **51**, 8545−8556.

57. F. G. Bordwell J. E. Bares, J. E. Bartmess, G. J. McCollumn, M. V. D. Puy, N. R. Vanier and W. S. Matthews, *J. Org. Chem*., 1977, **42**, 315-321.

58. J. D. Atwood, *Inorganic and Organometallic Reaction Mechanisms*, 2nd Ed., Wiley-VCH, New York, 1997, 749-771.

59. (a) M. L. Tobe and J. Burgess, *Inorganic Reaction Mechanisms*; Addison-Wesley Longman: Essex, England, 1999, 209-215 (b) R. G. Wilkins, *Kinetics and Mechanisms of Reactions of Transition Metal Complexes*; VCH: Weinheim, Germany, 1991, 136-151; (c) F. Basolo, *Coord. Chem. Re*v., 1996, **154**, 151-161.

60. A. Mandal, P. Karmakar, S. Mallick, B. K. Bera, S. Mondal, S. Ray and A. K. Ghosh, *J. Chem. Sci.,* 2012*,* **124**, 801-807.

61. A. Mandal, B. K. Bera, S. Mallick, S. Mondal, P. Karmakar and A. K. Ghosh, *Inorg. Chem. Indian J*., 2010, **5**, 176-180.

62. (a) B. M. Still, P. G. A. Kumar, J. R. Aldrich-Wright and W. S. Price, *Chem. Soc. Rev*., 2007, **36**, 665-686.

63. (a) E. Gabano, E. Marengo, M. Bobba, E. Robotti, C. Cassino, M. Botta and D. Osella, *Coord. Chem. Rev*., 2006, **250**, 2158-2174; (b) P. S. Pregosin, *Coord. Chem. Rev*., 1982, **44**, 247-291.

64. T. Soldatović, M. Shoukry, R. Puchta, Ž. D. Bugarčić and R. van Eldik, *Eur. J. Inorg. Chem*., 2009, 2261-2270.

65. P. O. Ongoma and D. Jaganyi, *Dalton Trans*., 2013, **42**, 2724-2734.

66. (a) H. Ertürk, R. Puchta and R. van Eldik, *Eur. J. Inorg. Chem*., 2009, **10**, 1331-1338; (b) H. Ertürk, J. Magut, R. Puchta and R. van Eldik, *Dalton Trans*., 2008, 2759-2766

67. P. O. Ongoma and D. Jaganyi, *Transition Met. Chem*., 2014, **39**, 407-420.

68. B. Petrovic, Ž. D. Bugarčić, A. Dees, I. Ivanovic-Burmazovic, F. W. Heinemann, R. Puchta, S. N. Steinmann, C. Corminboeuf and R. van Eldik, *J. Inorg. Chem*., 2012, **51**, 1516-1529; (b) E. C. Constable, C. Thompson, N. Armaroli, V. Belzani and M. Maestri *Polyhedron*, 1992, **11**, 2707-2709.

69. *C.* Maxim, A. Matni, M. Geoffroy, M. Andruh, N. G. R. Hearns, R. Clérac and N. Avarvari, *New J. Chem.*, 2010, **34**, 2319-2327.

70. M. C. Carrión, A. Guerrro, F. A. Jalón, B. R. Manzano and A. de la Hoz, *Inorg. Chem.*, 2003, **42**, 885-895.

71. A. Gelling, M. D. Olsen, K. G. Orrell, A. G. Osborne and V. Šik, *J. Chem. Soc., Dalton Trans.*, 1998, 3479-3488

72. G. A. Webb, *Nucl. Magn. Reson.*, 2009, **38**, 68-93.

73. A. Shaira and D. Jaganyi, *J. Coord. Chem.*, 2014, **67**, 2843-2857.

Kinetics and mechanistic study of polynuclear platinum(II) polypyridyl complexes; A paradigm shift in search of new anticancer agents

Panyako W. Asman*
School of Chemistry and Physics University of KwaZulu-Natal, 3209, Scottsville, Pietermaritzburg, South Africa
E-mail: pwangoli@yahoo.com

Graphical Abstract

In order to investigate the effect of the spacer groups adjacent to pyridyl N-donor, five ligands were synthesized and complexed with platinum to mimic cisplatin. Their reactivity with thiourea nucleophiles was carried out to shed light on their mechanistic insight. The study shows the differences in their reactivity to result from both electronic and steric effects arising in the tailoring of the bridging spacer.